NeuroImage 201 (2019) 116010

Contents lists available at ScienceDirect

NeuroImage

journal homepage: www.elsevier.com/locate/neuroimage

# The neurovascular response is attenuated by focused ultrasound-mediated disruption of the blood-brain barrier

Nick Todd [a,c,*], Yongzhi Zhang [a], Margaret Livingstone [b], David Borsook [c,d], Nathan McDannold [a]

[a] Department of Radiology, Brigham and Women's Hospital, Harvard Medical School, Boston, MA, USA
[b] Department of Neurobiology, Harvard Medical School, Boston, MA, USA
[c] Center for Pain and the Brain, Boston Children's Hospital, Harvard Medical School, Boston, MA, 02115, United States
[d] Department of Anesthesia, Perioperative, and Pain Medicine, Boston Children's Hospital, Harvard Medical School, Boston, MA, 02115, United States

ARTICLE INFO

*Keywords:*
Functional MRI
Hemodynamic response
Neurovascular response
Neurovascular coupling
Brain
Drug delivery
Neuroimaging
Somatosensory cortex

ABSTRACT

Focused ultrasound (FUS)-induced disruption of the blood-brain barrier (BBB) is a non-invasive method to target drug delivery to specific brain areas that is now entering into the clinic. Recent studies have shown that the method has several secondary effects on local physiology and brain function beyond making the vasculature permeable to normally non-BBB penetrant molecules. This study uses functional MRI methods to investigate how FUS BBB opening alters the neurovascular response in the rat brain. Nine rats underwent actual and sham FUS induced BBB opening targeted to the right somatosensory cortex (SI) followed by four runs of bilateral electrical hind paw stimulus-evoked fMRI. The neurovascular response was quantified using measurements of the blood oxygen level dependent (BOLD) signal and cerebral blood flow (CBF). An additional three rats underwent the same FUS-BBB opening followed by stimulus-evoked fMRI with high resolution BOLD imaging and BOLD imaging of a carbogen-breathing gas challenge. BOLD and CBF measurements at two different stimulus durations demonstrate that the neurovascular response to the stimulus is attenuated in both amplitude and duration in the region targeted for FUS-BBB opening. The carbogen results show that the attenuation in response amplitude, but not duration, is still present when the signaling mechanism originates from changes in blood oxygenation instead of stimulus-induced neuronal activity. There is some evidence of non-local effects, including a possible global decrease in baseline CBF. All effects are resolved by 24 h after FUS-BBB opening. Taken together, these results suggest that FUS-BBB opening alters that state of local brain neurovascular physiology in such a way that hinders its ability to respond to demands for increased blood flow to the region. The mechanisms for this effect need to be elucidated.

## 1. Introduction

Focused ultrasound (FUS) can achieve non-invasive and spatially localized disruption of the blood-brain barrier (BBB) (Hynynen et al., 2001). An ultrasound transducer with curved geometry for focusing transmits the acoustic pressure wave through the intact skull to a focal region in the brain that is several millimeters in extent. Gas-filled microbubbles are injected into the blood stream, and upon reaching the focal region they undergo a rapidly oscillating expansion and contraction in size known as stable cavitation. Forces created by cavitating microbubbles in the vessels leads to a local disruption of the BBB. The exact mechanisms for how normally non-BBB penetrant agents are then able to cross from the blood stream into the brain parenchyma are not fully understood. Research in animal models implicates greater transcellular permeability through widened tight junctions between endothelial cells, a reduction in drug efflux mechanisms, and an increase in the number of transcytotic vesicles (Aryal et al., 2017; Hynynen et al., 2005; Sheikov et al., 2008, 2004). The BBB remains permeable for several hours, and is fully resolved back to its original state within 24–48 h (Marty et al., 2012; Park et al., 2012). This powerful technology has been used for targeted delivery of a wide variety of therapeutics into the brain (Aryal et al., 2014; Burgess et al., 2015; Meairs, 2015; Timbie et al., 2015), including in clinical trials for Amyotrophic Lateral Sclerosis (NCT03321487), Parkinson's disease (NCT03608553), Alzheimer's disease (NCT02986932) and gliobastoma brain tumor (NCT03616860) patients (Lipsman et al., 2018; Mainprize et al., 2019).

* Corresponding author. 221 Longwood Avenue, EBRC, Rm 521, Boston, MA, USA.
*E-mail address:* ntodd1@bwh.harvard.edu (N. Todd).

https://doi.org/10.1016/j.neuroimage.2019.116010
Received 25 January 2019; Received in revised form 8 July 2019; Accepted 10 July 2019
Available online 11 July 2019

In addition to disrupting the BBB, several secondary physiological effects have been observed following the application of FUS with microbubbles. Raymond et al. demonstrated vasoconstriction in mice, showing an average reduction in vessel diameter of approximately 50% following the application of FUS (Raymond et al., 2007). The effect lasted approximately 5 min after which the vessels returned to their original diameter. A similar study performed in rats found that a much lower percentage of vessels showed signs of vasospasm (25% of vessels observed in rats vs 88% of vessels in mice) (Cho et al., 2011). Kovacs et al. reported that they measured significant elevation in several molecular and proinflammatory markers in rats after FUS-BBB opening. Levels of these markers remained elevated for up to 24 h and were interpreted to be indicative of a sterile inflammatory response (Kovacs et al., 2017). Evoked potential measurements and blood-oxygen level dependent (BOLD) functional MRI (fMRI) used during forepaw stimulation to investigate the effects on neuronal function in rats indicated that FUS BBB opening suppressed both the evoked potential measurements and the changes in the BOLD signal in response to the stimulus (Chu et al., 2015). The effect was only observed at higher ultrasound power levels that also lead to red blood cell extravasation seen on histology. Our group has shown that FUS-BBB opening, even at lower powers, breaks the functional connectivity between two interhemispheric cortical regions that usually exists in the rat brain, as measured by resting state BOLD fMRI (Todd et al., 2018).

All of these effects summarized above could have an impact on the working of the neurovascular unit, the group of interrelated cells involved in the function and energy supply of neuronal activity. It is comprised of neurons, astrocytes, endothelial cells that are a part of the blood-brain barrier, pericytes that are found on the surface of capillary vessels, and smooth muscle cells that surround pial and penetrating arterioles (Iadecola, 2017; Muoio et al., 2014). A main role of the neurovascular unit is to ensure the proper supply of oxygen and nutrients to all areas of the brain as local neuronal activity fluctuates up and down. This is achieved through the complex process of neurovascular coupling, where neuronal activity initiates a signaling mechanism to local blood vessels that in turn drives changes in vessel dilation or constriction to regulate blood flow to the region. Neurovascular coupling provides the rationale for using fMRI to study brain function, as changes in the BOLD signal measurable by MRI are assumed to be tightly coupled to neuronal activity. The full array of mechanisms that make up the neurovascular coupling process are still not well understood. An aggregation of evidence to date suggests that multiple signaling pathways exist from both neurons and astrocytes to the local vasculature, and that retrograde signaling through the vasculature propagates upstream via endothelial cells to induce vasodilation of larger arterioles and pial arteries (Iadecola, 2017).

In order to further understand the effects of FUS-BBB opening on neurovascular coupling, a series of experiments were carried out in rats consisting of FUS-BBB opening followed by fMRI imaging runs. BOLD and arterial spin labeling (ASL) fMRI data were collected to focus on the following questions about the effects of FUS-BBB opening: (i) are the vessels in a state of continuous dilation or constriction such that baseline cerebral blood flow would be altered? (ii) does it compromise the ability of vessels to react to signals for dilation, first from stimulus-induced neuronal activity and second from non-neuronal changes in blood oxygenation? (iii) is there a cortical-depth dependence to the effects seen, suggesting differences in how the hemodynamic response is altered for the capillary bed versus surface arterioles. It is important to understand these effects from a safety standpoint as FUS-BBB opening has entered clinical use. From a neuroscience standpoint, investigating the effects of this localized manipulation of the cerebrovascular network may provide insight into the mechanisms of neurovascular coupling.

## 2. Methods

### 2.1. Experimental design

This study contains three components: (1) The first was designed to characterize the effects of FUS-BBB opening on the hemodynamic response to an external stimulus as measured by BOLD and ASL fMRI. N = 9 Sprague Dawley rats underwent two days of experiments: sham FUS-BBB opening followed by anatomical and stimulus-based functional imaging on one day, and actual FUS-BBB opening followed by the identical imaging protocol on a separate day. (2) The second component used a hypercapnia gas challenge to determine if the effects of FUS-BBB opening on the BOLD signal are still present when the hemodynamic response is induced by a change in vessel blood oxygenation level as opposed to neuronal activity. An additional N = 3 Sprague Dawley rats underwent one experimental day consisting of FUS-BBB opening and BOLD imaging during a carbogen gas (95% O2, 5% CO2) breathing challenge. (3) The third component investigated whether the effects of FUS-BBB opening on the BOLD signal have a cortical-depth dependence to them. The same N = 3 Sprague Dawley rats from the second component also underwent high resolution stimulus-evoked BOLD fMRI. For all three components of the study the FUS-BBB opening was targeted to only the right hemisphere while the stimuli were applied bilaterally. To minimize the possibility of suppressing neuronal activity, the FUS BBB opening was done at a power level which was shown to not have an effect on evoked potential measurements (Chu et al., 2015) and histology was performed to confirm that no damage had been done to neuronal cells.

### 2.2. Animal preparation

All experiments and animal handling were performed under procedures approved by the Brigham and Women's Hospital Institutional Animal Care and Use Committee and in accordance with the Office of Laboratory Animal Welfare and the Association for Assessment and Accreditation of Laboratory Care regulations. Male Sprague Dawley rats were used for all experiments (242–334 g). Anesthetic induction was achieved with one dose of ketamine and xylazine (80 mg/kg/10 mg/kg) at the start of each experiment. The head of the rat was shaved and depilatory cream was applied to remove all fur for optimal ultrasound coupling. A tail vein catheter was inserted to be used for injections of microbubbles and MRI contrast agent.

### 2.3. FUS blood-brain barrier opening

FUS-BBB opening was targeted to the somatosensory cortex (S1) in the right hemisphere. The procedure was performed with an in-house made MRI-compatible focused ultrasound system. The ultrasound transducer operates at 690 kHz and has a 3.0 cm diameter and 3.5 cm radius of curvature. The system additionally has a three-axis manual positioning system to move the transducer, a single element passive cavitation detector, and a transmit/receive MRI RF coil. The rat lies supine with its head fixed in place by ear bars and coupled to the ultrasound transducer by a bath of degassed water. The FUS sonications are generated by a function generator (33220A, Agilent), amplifier (240L, E&I) and custom Matlab user interface. Accurate targeting of the right S1 region was achieved by steering the location of the FUS focal point (as determined by a pre-setup heating of a silicone gel phantom) to the location of S1 (as determined from an MRI T2-weighted structural image of the brain).

BBB opening was done by applying repeated bursts of FUS sonications immediately after injection of microbubbles (200 μL/kg bolus injection of Optison, GE Healthcare). The sonication parameters were 10 ms bursts, 1 Hz repetition frequency, and 120 repeats. To ensure full coverage of the right S1 region, five sets of sonications were applied over a 2 × 2 mm square (4 corners and one in the middle), with the center of the focus targeted to 1 mm below the cortical surface. All sonications were applied at a peak negative pressure of 0.34 MPa (as calibrated in water), which is estimated to correspond to a pressure of 0.26 MPa in the brain after accounting for a 23% attenuation loss due to transmission through the skull (O'Reilly et al., 2011). The frequency spectra of measurements recorded from the passive cavitation detector were used to

monitor microbubble activity (McDannold et al., 2006). An increase in the magnitude of the first harmonic is indicative of microbubble stable cavitation, which was seen in all sets of sonications in all rats. The presence of a broadband increase in the acoustic emission signal is associated with inertial cavitation, a violent collapse of microbubbles that leads to tissue damage, which was not seen in any of the rats. A warming blanket was used throughout the BBB opening process to maintain body temperature and the rat's breathing was continuously monitored. For sham BBB opening, the rat was positioned in the FUS system and water bath for an equivalent amount of time, but no FUS sonications were applied.

After all of the fMRI runs were completed, the extent of BBB opening was assessed using contrast enhanced imaging. T1-weighted images were acquired before and after tail vein injection of gadolinium (Magnevist, 0.25 mL/kg) and converted to percent difference. The RARE sequence parameters were: 0.3 x 0.3 × 0.6 mm resolution; 18 slices with 0.4 mm slice gap; TR = 609 ms; TE = 18 ms. The percent difference images were co-registered to the anatomical image and normalized into template space (as described below).

### 2.4. Functional MRI

The imaging was performed over approximately 1 h and 20 min, starting approximately 1 h after the completion of the ultrasound sonications for BBB opening. After BBB opening, the rat was removed from the FUS system and set up in the conventional Bruker animal holder, all the while kept in an unconscious state. A nose cone was used for delivery of isoflurane and oxygen, body temperature was maintained with a water warming blanket, and a 2 cm surface coil was place over the rat's head for signal acquisition. The rat's breathing rate was monitored throughout the experiment. A bolus injection of Dexdomitor was given subcutaneously (Dexmedetomidine; Orion, Espoo, Finland; 0.025 mg/kg) and delivery of 0.25% isoflurane in 60% oxygen was started (Adamczak et al., 2010). Periodic infusions of Dexdomitor were given as needed to keep the rat in a stable physiological state. This combination of medetomidine and light isoflurane has been shown to be beneficial for functional imaging studies of sedated animals (Brynildsen et al., 2017).

Bilateral activation of the hind limb region of the somatosensory cortex was achieved by electrical stimulation of the rat's hind paws. Pairs of 30 gauge needles were inserted into the pads of the second and fourth digits on each hind paw. Electrical pulses of 300 ms duration were delivered at 6 Hz using a TENS unit (TU 7000, Tensunits.com, Largo, Florida) connected to an in-house built circuit that synchronized the stimulus to the MR data acquisition. The voltages in each branch of the circuit going to the two hind paws were measured on an oscilloscope and adjusted to have equal values of 600 mV as measured across a 177 Ω resistor in series with the circuit, corresponding to approximately 3 mA of current to each hind paw.

The fMRI imaging for the first component of the study consisted of four imaging runs using block-designed stimuli: short (6 s On, 84 s Off) and long (18 s On, 72 s Off) stimulus durations were imaged with a BOLD sequence and an ASL sequence. The BOLD fMRI data was acquired with a 2D single-shot gradient echo echo-planar imaging (EPI) sequence. Sequence parameters were: 3.2 × 3.2 cm field of view; 64 x 64 x 18 imaging matrix; 0.5 x 0.5 × 1.2 mm resolution; 18 1.0 mm axial slices with 0.2 mm slice gap; TR = 1500 ms; TE = 18 ms; four dummy scans prior to data acquisition; 325 image volumes acquired in 8 min and 8 s. The ASL data was acquired with a 2D single-shot continuous ASL sequence. Sequence parameters were: Interleaved tag/control images; TR = 3000; TE = 16.5; 1 axial slice (2 mm thick); 3.2 × 2.4 cm field of view; 64 x 48 x 1 imaging matrix; 0.5 x 0.5 × 2.0 mm resolution; 2000 ms labeling duration; 350 ms post-label delay; 164 images acquired in 8 min and 12 s. The single axial slice of the ASL scan was placed to be in the center of the hind limb region of the somatosensory cortex.

The fMRI imaging for the second component of the study used the same BOLD sequence as in the first component, but the stimulus was replaced by a hypercapnic gas challenge. The breathing of carbon dioxide is known to stress the cerebral vascular system and cause a vasodilatory effect. But unlike the hind paw stimulation studies done above, any changes in hemodynamics will not have been initiated from a neuronal activity source. During imaging, the gas delivery was alternated from medical air (79% N, 21% O2) for 3 min to carbogen (95% O2, 5% CO2) for 1 min, repeated three times. The rat was acclimated to breathing medical air for at least 10 min before imaging began (with the same level of 0.25% isoflurane as before). The imaging parameters were the same as those used in the first component of the study described above, except 525 image volumes acquired in 13 min and 7 s.

The fMRI imaging for the third component of the study consisted of one imaging run using a high resolution single-shot EPI BOLD sequence and the short duration block-designed stimulation (6 s On, 84 s Off). Sequence parameters were: 2.5 × 2.5 cm field of view; 100 x 75 x 12 imaging matrix (3/4 partial Fourier in the phase encode direction); 0.25 x 0.25 × 1.2 mm resolution; 18 1.2 mm axial slices with no slice gap; TR = 1000 ms; TE = 18 ms; four dummy scans prior to data acquisition; 488 image volumes acquired in 8 min and 8 s.

For all imaging sessions, the main field homogeneity was optimized using the Bruker MAPSHIM protocol and an anatomical image was acquired with a T2-weighted RARE sequence (0.3 x 0.3 × 0.5 mm resolution; 60 slices with no slice gap; TR = 6500 ms; TE = 50 ms).

### 2.5. BOLD data analysis

All BOLD fMRI images were pre-processed using SPM12 (2014) and custom Matlab scripts. To assess the location and extent of stimulus induced activation, the data were analyzed in terms of percent change in the BOLD signal. The T2-weighted anatomical image was segmented in SPM12 using the template of Valdes-Hernández et al. (Valdés-Hernández et al., 2011). The EPI images were realigned, co-registered to the anatomical image, normalized to the template space, and spatially smoothed with a Gaussian filter of 0.8 x 0.8 × 0.8 mm FWHM. The data sets were further processed with a temporal high-pass filter (0.0056 Hz) and the time signal spatially averaged over a white matter mask was regressed out. The signal was converted into percent change from the non-stimulus baseline and averaged over stimulation blocks to produce an average signal over the 90 s on/off stimulation block.

Time courses of the percent change in the BOLD signal were extracted from the left and right hindpaw S1 regions. An ellipsoidal cylinder shape was used for the ROI with dimensions, 1.75 × 2.5 mm in the cortical plane and 1.5 mm through the cortex. The location in the cortical plane was determined using each individual rat's peak of activation, as defined by the center-of-mass of the BOLD signal change 6 s into the stimulation block. Locations of the individual ROIs did not vary more than [ ±0.5 mm, ±0.5 mm] over all data sets. The data was spatially averaged over these ROIs and the plots are presented as the mean over the nine rats, with shaded regions depicting±one standard deviation over the nine rats. Tests for significant differences in the BOLD signal change between the left and right S1 regions were done at each time point in the stimulus block using a two-tailed *t*-test and Bonferroni corrected for 60 multiple comparisons.

Due to the single slice acquisition, the ASL data was not realigned, coregistered or normalized into the template space. Coregistration was based solely on the original positioning of the slice during the time of acquisition. The data was spatially smoothed with a Gaussian filter of 1.0 x 1.0 × 1.0 mm FWHM and then converted into estimates of cerebral blood flow (CBF). To minimize BOLD weighting of the data, the subtraction of the tagged images from the controls was done following the procedure of Chuang et al. (2008). The time series data were high pass filtered (>0.083 Hz) to remove the BOLD signal fluctuations and then demodulated by multiplying by cos(π*n) to retain both the baseline CBF and the changes in CBF due to stimulation. Conversion to CBF was done according to (Alsop et al., 2015):

$$CBF = 6000 \cdot \frac{SI_C - SI_L}{SI_C} \cdot \frac{\lambda \cdot R_1}{2\alpha \cdot e^{(\min(\delta - PLD, 0) \cdot R_1)} - e^{(-(\tau + PLD) \cdot R_1)}}$$

6000 is a scaling factor to convert the units into ml/100 g/min, $SI_C$ is the signal intensity from the control scan, $SI_L$ is the signal intensity from the labeled scan, $\lambda = 0.9$ is the blood-tissue partition coefficient, $R_1 = 0.625\ s^{-1}$ is the assumed T1 relaxation rate of gray matter tissue, $\alpha = 0.85$ is the labeling efficiency, $\delta = 0.3$ s is the assumed arterial transit time, $PLD = 0.35$ s is the post-label delay time, and $\tau = 2.0$ s is the labeling duration.

As with the BOLD analysis, time courses of the CBF signal were extracted from the left and right S1 regions and averaged over the stimulation blocks. ROIs of 1.5 x 1.5 × 2.0 mm were used, centered on the peak of CBF change. Tests for significant differences in the CBF change values between the left and right S1 regions were done at each time point in the stimulus block using a two-tailed *t*-test and Bonferroni corrected for 30 multiple comparisons.

Maps of the baseline CBF values were calculated using only data from the last 30 s of the 90 s stimulation blocks, when any changes in CBF had returned to baseline. Data from these time points were averaged to create a single baseline CBF map for each rat. Tests for significant differences in the baseline CBF values between the left and right S1 regions were done with a two-tailed *t*-test.

### 2.6. Hypercapnia data analysis

The BOLD data acquired during the hypercapnia study underwent realignment, co-registration to the anatomical image, normalization into the template space, and spatial smoothing with a Gaussian filter of 0.8 x 0.8 × 0.8 mm FWHM. High pass filtering was not done due to the very slow time course of the air/carbogen blocks (4 min = 0.0042 Hz). Regression of the average white matter signal was not done due to the widespread changes in signal throughout the brain caused by the hypercapnic challenge. The data were converted into percent signal change using the average of the medical air blocks as the baseline. ROIs of the same size as in the first component of the study were used to obtain a signal time course that was averaged over the three air/carbogen blocks. The ROI for the right hemisphere was chosen to align with the center of the BBB opening, and the ROI for the left hemisphere was placed contralaterally in the same cortical region.

### 2.7. High resolution BOLD data analysis

The high-resolution BOLD data was processed in the same manner as the normal resolution BOLD data described above, with the important exception that the smoothing kernel used had 1.0 x 0.1 × 1.0 mm FWHM. This imparted essentially no smoothing in the cortical depth direction, but still smoothed the data within the cortical plane to improve SNR lost from the smaller voxel size. ROIs for the left and right S1 regions were determined in the same manner as described above. For the plots of the time courses, the data was averaged over the entire ROI. For the plots of BOLD signal as a function of cortical depth, the data was taken from the time point 6.5 s after stimulus onset and averaged over the ROI within each individual cortical plane. This created nine data points spanning 2.25 mm of cortical distance.

### 2.8. Histology

To assess signs of tissue damage due to the FUS-BBB opening, histology was performed on each of the nine rats from the first component of the study. The rats were sacrificed one (N = 4), two (N = 2), three (N = 2), or seven (N = 1) days after FUS sonication. The brains of the rats were perfused with saline solution (100 mL, 0.9% NaCl) and 10% buffered formalin (100 mL), fixed in 10% buffered formalin phosphate, and cut into axial blocks embedded in paraffin. The blocks were sectioned into 5 μm thick slices and stained with Haematoxylin and Eosin (H&E). A neurobiologist with over 20 years of experience examined the stained slides to determine the presence of damage to neuronal or other tissues. All slides covering the cortex were considered, with particular attention paid to the brain region where FUS-BBB opening occurred as determined by the contrast MRI images.

## 3. Results

### 3.1. BBB opening

The location of BBB opening was confined to the right hemisphere in all nine rats, occurring primarily in the region of the somatosensory cortex (Fig. 1). Despite using fixed ultrasound parameters, the extent of BBB opening varies across the nine rats. This is likely due primarily to differences in skull geometry and orientation relative to the transducer and secondarily to other aspects of biological variability such as vessel size and distribution. The histology performed on the rats indicated that the ultrasound did not cause damage to local tissue. There were no signs of extravasation of red blood cells and no indications of injury to neuronal cells.

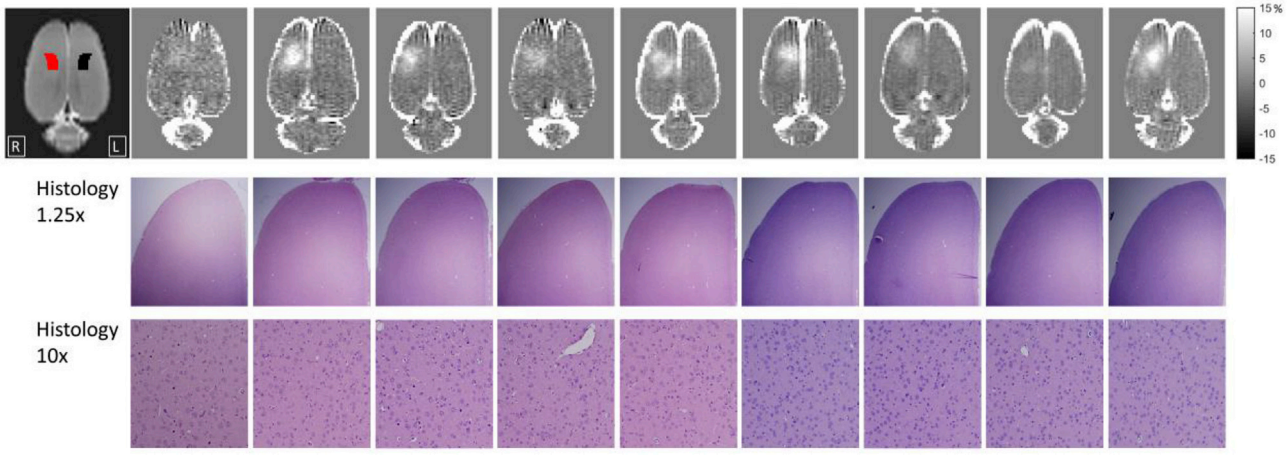


**Fig. 1.** Summary of FUS-BBB opening and histology results. The top row shows T1-weighted contrast images depicting the location and extent of BBB opening for all nine rats (images shown as percent change pre-to post-contrast agent injection). The location of the right (red) and left (black) S1 hind limb regions according to the Paxinos and Waston rat brain atlas (Paxinos and Watson, 2013) are shown overlaid on the T2-weighted image at the far left. Histology of H&E stained slides of the targeted right cortex are shown at 1.25x and 10x magnification. No signs of damage to cells or extravasation of red blood cells was seen for any of the rats.

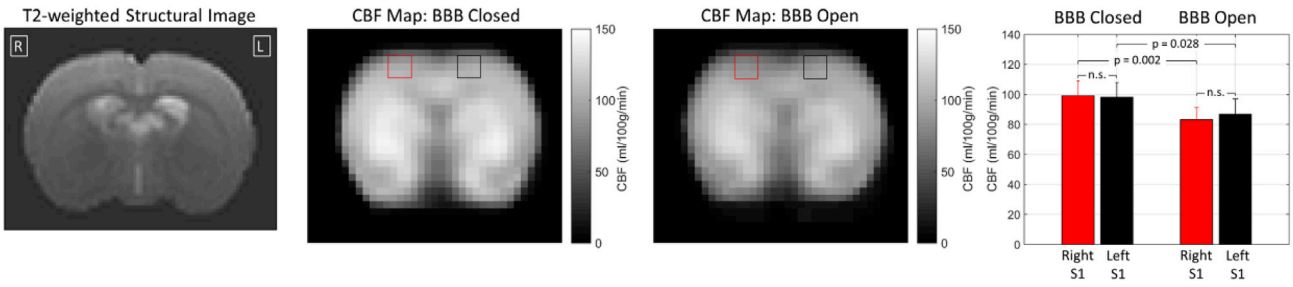


**Fig. 2.** Baseline CBF results. Maps of CBF values in the single slice acquired through the somatosensory cortex for the conditions of BBB closed and BBB open. The data is the mean over the N = 9 rats. A T2-weighted anatomical image is shown for reference. The red and black squares on the CBF maps indicate the left and right S1 ROIs that were used in the bar plot at the far right (mean and standard deviation over nine rats). The p-values are based on a two-tailed *t*-test without correction for multiple comparisons (n.s. = not significant).

### 3.2. Effects of FUS-BBB opening on baseline CBF

Measurements of the baseline CBF for the rats in the BBB closed and BBB open conditions are shown in Fig. 2. These values indicate the rate of perfusion in the rat brain at rest-i.e., absent any activation due to stimulation. The bar plots show the average CBF values in the left and right S1 regions. Within the conditions of BBB closed and BBB open, there are no differences in baseline CBF between the left and right S1 regions. Comparing between conditions, the CBF values were generally higher for the condition of BBB Closed, by approximately 10% on average. The t-tests performed indicate that both the left and right S1 regions had significantly higher CBF values for the condition of BBB Closed. When the CBF values were averaged over the entire slice, the difference was not significant, and nor were there significant differences for any individual voxels outside of the S1 ROIs.

### 3.3. Effects of FUS-BBB opening on stimulus-based changes in BOLD and CBF

The results from the BOLD stimulus-based fMRI runs are shown in Figs. 3 and 4. The data from the BBB closed condition confirms that the BOLD responses in the left and right hemispheres are not significantly different in terms of either amplitude or duration, and that the rise in BOLD signal lasts longer for the 18 s stimulus, as expected. For the condition where the BBB has been opened, the response in the targeted right S1 is significantly decreased in both amplitude and duration. The initial rise of the BOLD signal is not delayed, but it does not reach the same peak amplitude and it returns to baseline more quickly. In the case of the 18 s stimulus duration, the return to baseline happens even while the stimulus is still on. There also does not appear to be a post-stimulus undershoot for the BBB open cases, as there is when the BBB is closed.

As seen in Fig. 3, the mean BOLD signal change is larger in the left S1 region during BBB Open compared to BBB Closed for both the 6-s stimulus data (peak change of 5.8% vs 4.5%) and 18-s stimulus data (peak change of 6.4% vs 4.1%). However, tests for significant differences in the data over all time points do not survive correction for multiple comparisons, either using the stringent Bonferroni correction or the less strict false discovery rate correction.

The BOLD data was analyzed to investigate whether the observed effect of BOLD signal change attenuation was correlated with the extent of BBB opening. The results are shown in Supplementary Figure 1. There is no evidence of such a correlation for the 6-s stimulation data, however there is reasonably strong evidence that such a correlation exists in the 18-s stimulation. For the 18-s data the correlation is strongest towards the end of the stimulus-on time. While the correlation values do not exceed the stringent significance criteria of $p < 0.05$ corrected for multiple comparisons, several time points do cross the threshold of $p < 0.01$ uncorrected.

Fig. 4 shows a direct comparison of time courses for the 6 s and 18 s stimulus durations from the right and left S1 regions for the BBB open condition. For the targeted right S1 region, the time courses of the BOLD signal change show a similar pattern for both stimulus durations. In the non-targeted left S1 region, the result of longer lasting BOLD change for the longer stimulus duration are in line with what would be expected.

Results showing the changes in CBF in response to the stimulus are shown in Fig. 5. The format is the same as in Fig. 3, where CBF time courses are shown for the left and right S1 region at both stimulus durations and under conditions of BBB closed and BBB open. As with the BOLD results, the BBB closed condition confirms the expectation of changes in CBF that are similar for the left and right S1 regions, and a longer lasting change when the stimulus duration is longer. Unlike the BOLD results, when the BBB is open the change in CBF in the targeted right S1 region is not merely attenuated but appears to be completely suppressed.

To determine the duration of the effect, one rat from the group of nine was additionally imaged 1, 3, and 7 days after BBB opening. The BOLD and CBF results from these four days are shown in Fig. 6. As with the group results, there is a clear attenuation of the BOLD signal change and a complete suppression of the CBF signal change on the day of BBB opening. One day later, the time courses for the changes in BOLD and CBF are similar in amplitude and duration between the left and right S1 regions. The BOLD and ASL time courses for the left and right regions remain very similar on days 3 and 7, suggesting that the effect of BBB opening is resolved after 24 h and no lingering effects remain several days later.

### 3.4. Effects of FUS-BBB opening on vessel reactivity to changes in blood oxygenation

Three additional rats underwent BBB opening and standard resolution BOLD imaging during a gas challenge scan that alternated the gas mixture fed into the nose cone between medical air (78% Nitrogen and 21% oxygen) and carbogen (95% oxygen and 5% carbon dioxide). Plots of the BOLD signal time course and corresponding maps of the BOLD change at various time points are shown in Fig. 7. In the first rat, there is a small difference in the BOLD signal time course between the targeted right hemisphere and the non-targeted left hemisphere. In the second and third rats, there is a clear reduction in the amplitude of the BOLD change in the targeted right hemisphere caused by the carbogen breathing. It does not appear that the duration of the BOLD change is affected, as it was in the stimulus studies above. The BOLD signal in the right hemisphere "catches up to" the signal from the left hemisphere and they both return to baseline at the same time.

### 3.5. Cortical depth dependence of BOLD changes

The same three rats as used in the carbogen experiments also underwent stimulus-evoked fMRI with high resolution BOLD imaging using only the 6 s stimulus duration. An analysis of possible effects on the BOLD signal related to cortical distance is presented in Fig. 8. The results for

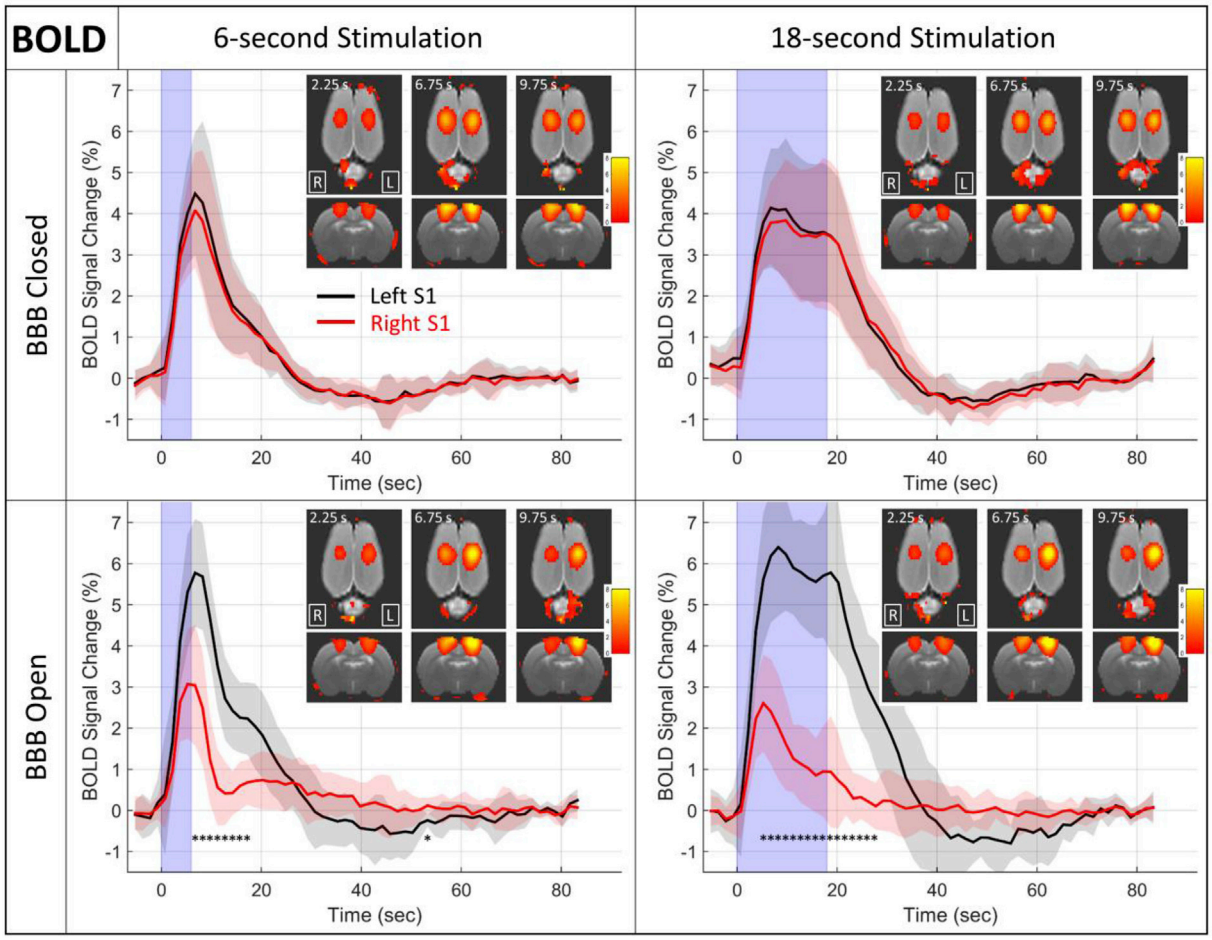


**Fig. 3.** BOLD results. Plots of the percent change in the BOLD signal in response to hind paw stimulation are shown for the left (black) and right (red) S1 regions. The solid line is the mean over all N = 9 rats and the shaded regions depict±the standard deviation over the nine rats. The light blue shading represents the time that the stimulus is on. Inset images show coronal and axial views of BOLD change maps at three time points after the stimulus onset. * indicates time points in the stimulus block where the BOLD signal change is significantly different between the left and right S1 regions (two-tailed *t*-test, Bonferroni corrected for 60 multiple comparisons, $p < 0.05$). No significant differences were seen for either of the BBB Closed cases.

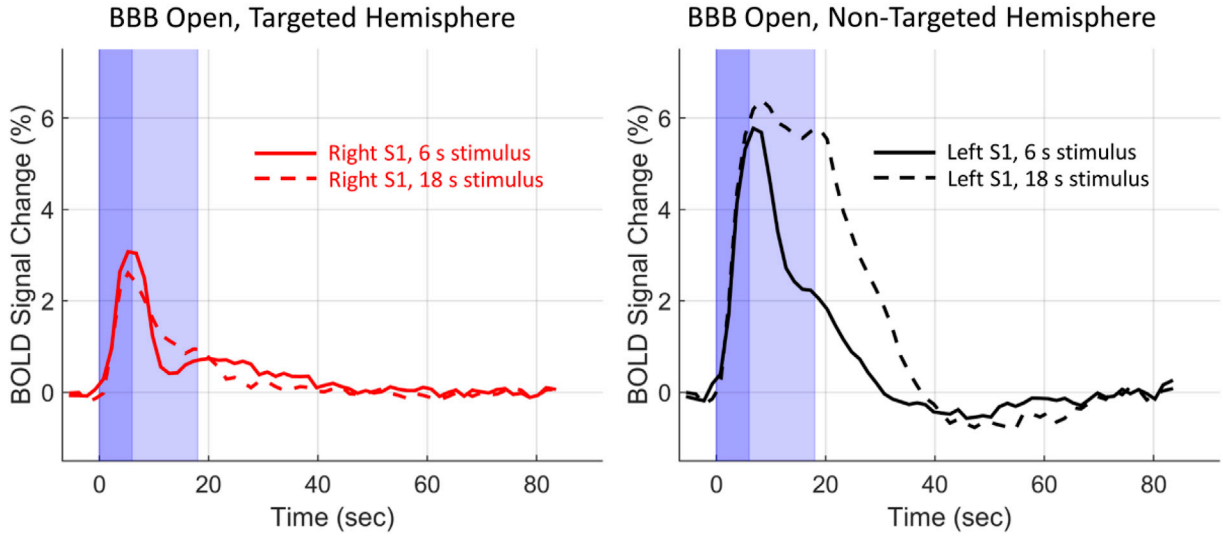


**Fig. 4.** Comparison of short and long duration BOLD time courses. Mean of BOLD time courses for 6 s (solid lines) and 18 s (dashed lines) stimulus durations are plotted together. The time courses from the right S1 region (red) are very similar despite the different stimulus durations. The time courses from the left S1 region (black) are in line with expectations, with the BOLD signal remaining elevated longer for the longer stimulus duration.

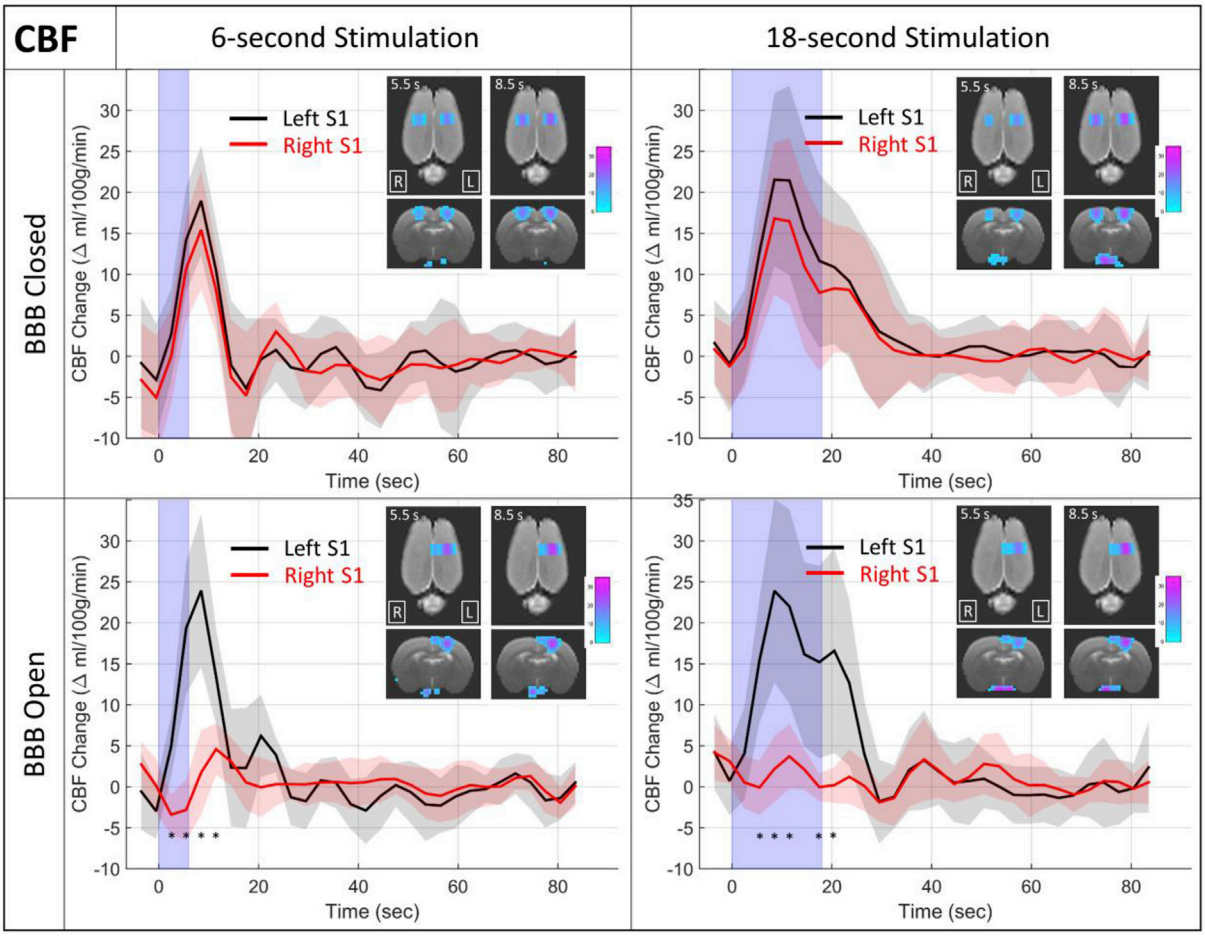


**Fig. 5.** CBF change results. Plots of the change in CBF in response to hind paw stimulation are shown for the left (black) and right (red) S1 regions. The solid line is the mean over all N = 9 rats and the shaded regions depict±the standard deviation over the nine rats. The light blue shading represents the time that the stimulus is on. Inset images show coronal and axial views of CBF change maps at two time points after the stimulus onset. * indicates time points in the stimulus block where the CBF change is significantly different between the left and right S1 regions (two-tailed *t*-test, Bonferroni corrected for 30 multiple comparisons, $p < 0.05$). No significant differences were seen for either of the BBB Closed cases.

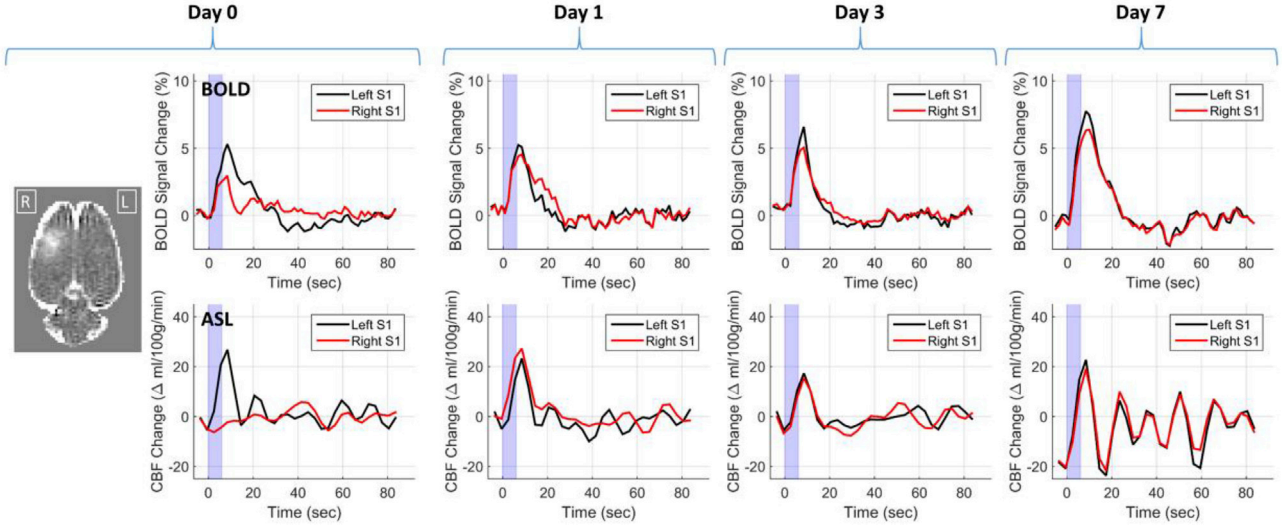


**Fig. 6.** Duration of effects. BOLD and CBF time courses from one rat on the day of BBB opening, and 1, 3, and 7 days later. The T1-weight contrast difference image at the far left shows the extent of BBB opening for this rat. The plots show changes in BOLD and CBF for the left (black) and right (red) S1 regions in response to a 6 s stimulus.

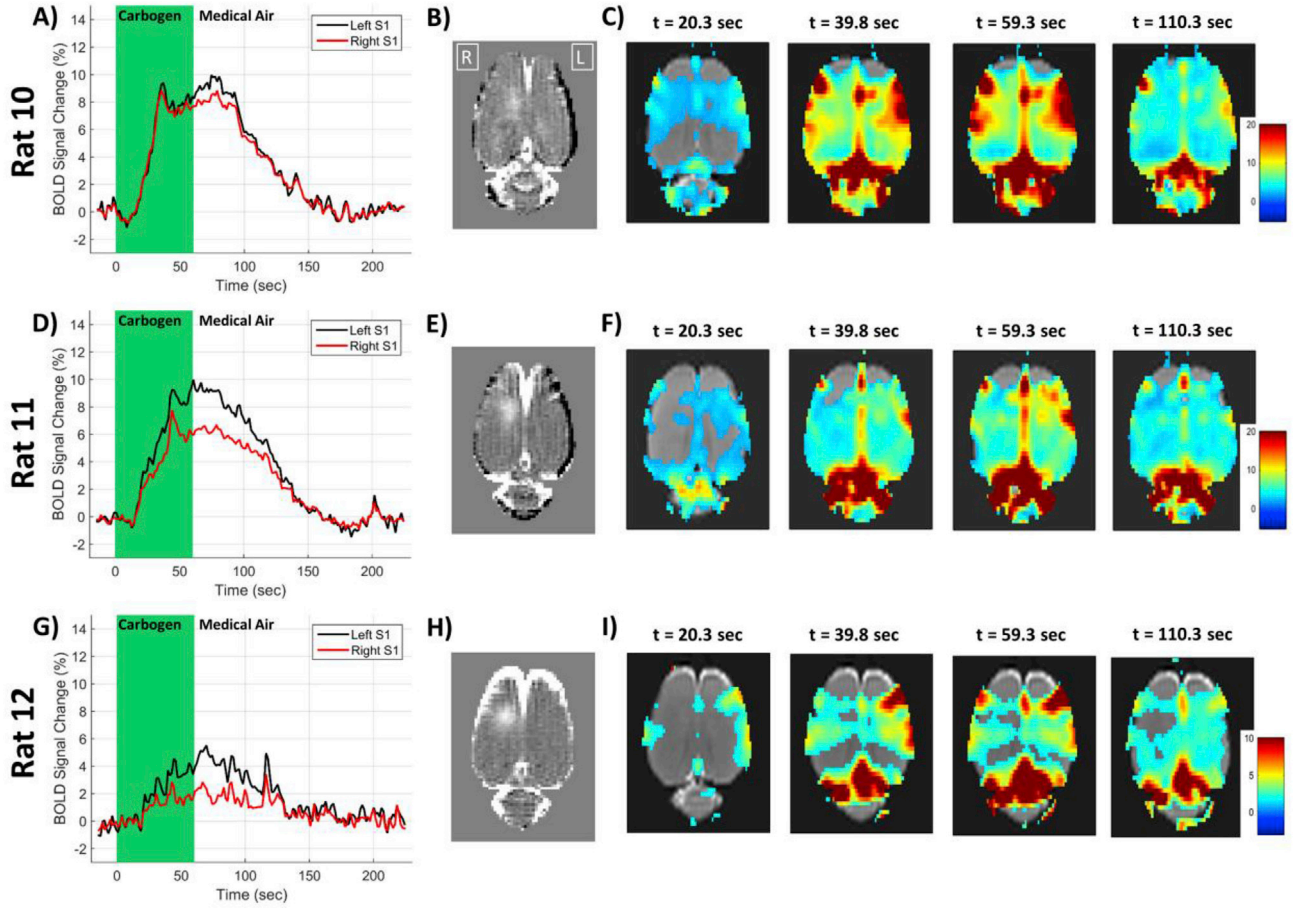


**Fig. 7.** Carbogen gas challenge BOLD results. Individual results from three rats are shown in the three rows. The first column shows plots of the BOLD signal changes in the left (black) and right (red) cortical regions. The second column shows the T1-weighted contrast difference image of the BBB opening. The images in the last four columns are maps of percent change in the BOLD signal at different time points after the initiation of carbogen breathing. Note that the color scale of the BOLD percent change is reduced to only 0–10% for Rat 12 due to the smaller change seen.

each individual rat show the extent of BBB opening, the BOLD signal change time courses for the left and right S1 regions, plots of the BOLD signal change as a function of cortical distance from white matter for the left and right S1 regions (at 6.5 s after stimulus onset), and maps of the BOLD signal change at three difference cortical distances (also at 6.5 s after stimulus onset). The origin for the cortical distance analysis is at the white matter – gray matter interface with distances increasing towards the cortical surface. In all three rats the non-targeted left S1 region shows a clear relationship of greater BOLD signal changes towards the cortical surface, as has been demonstrated by others (Tian et al., 2010). This relationship holds for the targeted right S1 region in one rat, but in the other two rats the rise in BOLD signal change plateaus at the highest cortical layers.

For comparison, a similar analysis of BOLD signal change as a function of cortical distance was performed using the lower resolution BOLD data from the nine rats in the first component of this study. The data were reprocessed using the same 1.0 x 0.1 × 1.0 mm FWHM smoothing kernel as was used for the high-resolution BOLD data. The individual plots of BOLD signal change as a function of cortical depth are shown in Supplementary Figure 2 for the conditions of BBB closed and BBB open.

## 4. Discussion

The aim of this study was to further elucidate the effects that FUS-mediated disruption of the BBB has on neurovascular physiology. Our main findings can be summarized as follows: (1) FUS-BBB opening attenuates the neurovascular unit's ability to respond to demands for increased blood flow. This was shown to be the case when the initiating mechanism was local stimulus-evoked neuronal activity and when it was global changes to blood oxygenation. The attenuation in the neurovascular response was present for both short and long duration stimuli. It is not clear which mechanism in the cascade of events that make up the neurovascular response is responsible for the effect. It could be any one of neuronal activity, neurovascular signaling, the local vasculature, or retrograde vascular signaling mechanisms that recruit increased flow from upstream vessels. (2) There is some marginal evidence that targeted FUS-BBB opening leads to non-local reductions in baseline CBF values. There is more convincing evidence that following FUS-BBB opening to one hemisphere, the baseline CBF values are not different between the targeted and non-targeted hemispheres. (3) These changes are transient, lasting less than 24 h, and no tissue damage was observed on histology, implying that discernable damage to tissue due to the FUS plus microbubbles is not the cause. Whatever underlying physiology is altered by FUS-BBB opening, those changes appear to be completely reversible.

### 4.1. Which components of the neurovascular unit are affected?

In the sequence of events that constitute the neurovascular response, neuronal activity leads to neurovascular signaling which leads to a vascular response. If any of these components were affected by FUS-BBB opening, the effect would propagate to the cerebral hemodynamics and blood flow that were measured in this study. It is unlikely that neuronal activity was suppressed by the BBB opening. Chu et al. showed that when FUS is applied using a mechanical index of 0.55 (400 kHz, 0.35 MPa),

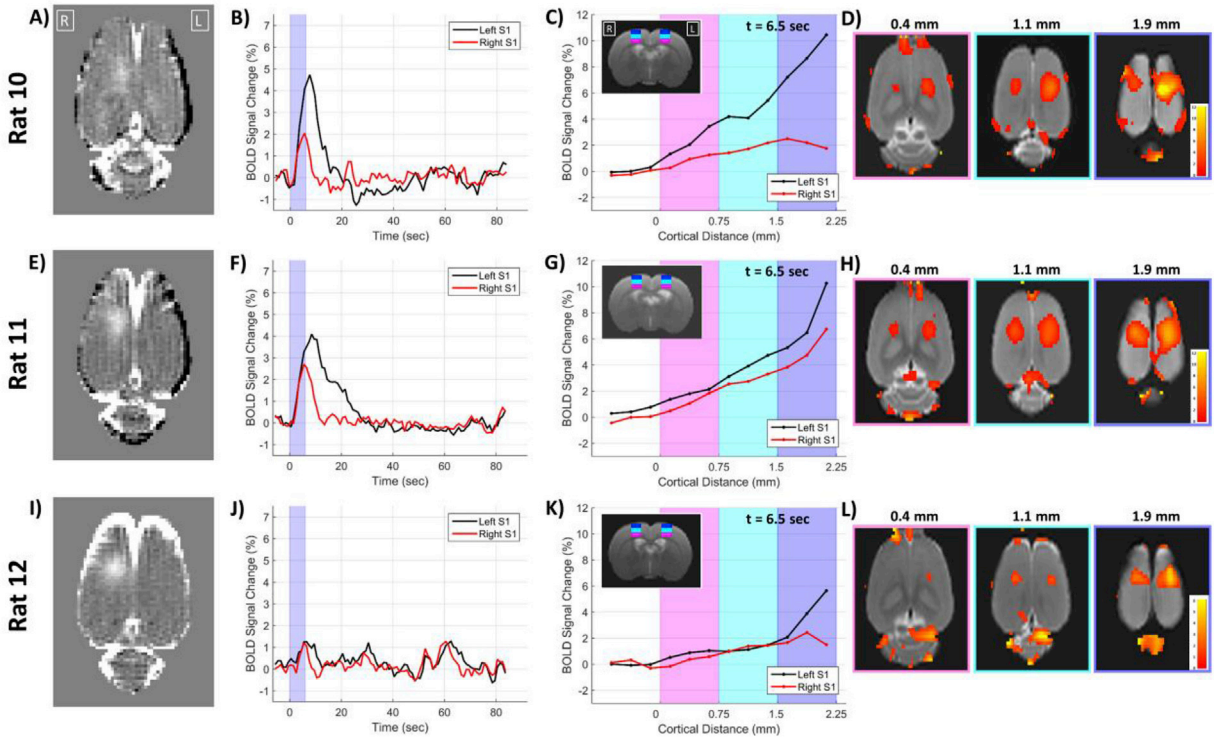


**Fig. 8.** Cortical depth BOLD results. Individual results from three rats are shown in the three rows. The first column shows the T1-weighted contrast difference image of the BBB opening. The second column plots the BOLD signal change time courses for the left and right S1 regions. The third column plots the BOLD changes at 6.5 s after stimulus onset as a function of cortical depth. The locations of the shaded magenta, cyan and blue regions on the plots are shown on the T2-weighted anatomical image inset. The fourth column shows maps of BOLD signal from 6.5 s after stimulus onset at three different cortical distances from white matter.

there are no changes to the amplitude or latency of the P1 peak of a somatosensory evoked potential measurement at 60 min after BBB opening (Chu et al., 2015). In our study, we used FUS parameters that give a lower mechanical index of 0.41 (690 kHz, 0.34 MPa) and performed imaging between one and 2 h after BBB opening.

It is possible that one of the many neurovascular signaling pathways are affected by BBB opening. One explanation would be that the upregulation of pro-inflammatory molecules see by Kovacs et al. could have an interfering effect on the molecular messengers that are released after neuronal activation to mediate dilation and constriction of surrounding vessels (Kovacs et al., 2017). In the work reported by Kovacs et al., the effects persisted for only several hours and largely returned to baseline by 24 h later. However, that study used a higher microbubble dose and had a much larger area of BBB opening than our study, which could potentially lead to significantly different effects between their experiments and ours.

If neither neuronal activity nor neurovascular signaling were affected by the BBB opening, then the observed effects must be due to physiological changes in the vasculature itself. This could either be changes in the capillary vasculature that is closest to the neuronal activity and known to be most affected by FUS-BBB opening, or it could be disruptions in the hypothesized retrograde signaling that occurs along vessel endothelial cells in order to initiate dilation in upstream arterioles and pial surface vessels.

### 4.2. The ability of the vasculature to respond following BBB opening

Both the BOLD and the CBF data confirm that FUS-BBB opening attenuates the hemodynamic response to an external stimulus. This finding was also observed in the Chu et al. paper using BOLD measurements at 1 h after opening with slightly stronger FUS parameters (0.35 MPa peak negative pressure, 0.55 Mechanical Index) (Chu et al., 2015). In our data shown in Fig. 3, the BOLD signal change onset time does not appear to be affected. But the amplitude and duration of the BOLD change are clearly diminished. In the case of the longer duration 18 s stimulus, the BOLD change is returning towards baseline even while the stimulus is still on. It is also interesting that a clear sign of post-stimulus undershoot is seen in all of the data where the BBB is closed, but not so for the two cases where the BBB is open. Finally, it is possible that the BOLD response time courses in areas of BBB opening are independent of stimulus duration. Only two stimulus durations were tested, but the time courses for the 6 s and 18 s stimuli appear very similar (Fig. 4).

The effects of BBB opening are even more striking in the CBF data (Fig. 5). Based on these measurements, it appears that there is essentially no change in blood flow in response to the stimulus. The average time course from the 6 s stimulus data looks as if there might be an initial drop in flow at the stimulus onset followed by a delayed small peak. However, these changes are small enough that they could very well be just noise.

It is difficult to reconcile the fact that there is an observed change in BOLD but no observed changes in blood flow based on the CBF measurements. The hemodynamic response that gives rise to changes in the BOLD signal is understood to be driven by changes in flow. For example, the balloon model of BOLD signal changes proposed by Buxton et al. is a set of coupled differential equations that rests on changes in flow into the tissue (Buxton et al., 1998). If there are no changes to flow, then there are no changes in venous blood volume, no changes in the concentration of deoxyhemoglobin, and no changes in the BOLD signal. It is possible that the answer lies with two other parameters known to affect the BOLD signal that were not measured in this study: the cerebral metabolic rate of oxygen consumption and the local tissue blood volume. The cerebral metabolic rate of oxygen consumption is modelled as the product of oxygen extraction, arterial oxygen content and cerebral blood flow.

The carbogen gas challenge experiments provided a way to induce vessel reactivity from a source that was not neuronal activity. If the left and right cortical regions responded in a similar manner that would be strong evidence that the effects seen in the stimulus-evoked BOLD and CBF data were due to alterations in either neuronal activity or

neurovascular signaling mechanisms. However, BBB opening did have an effect on the changes in the BOLD signal (Fig. 7). As with the stimulus-evoked response, the onset of the change does not seem to be altered, but the peak amplitude of the change is reduced. Unlike the stimulus-evoked results, the BOLD signal does not make a quicker return to baseline. The time course of the right S1 region "catches up" to the left S1 time course and they both reach the return to baseline at the same time. These results indicate that the diminished ability of the vasculature to respond to demands for increased flow is at least partly due to changes in the physiology of the vascular itself, and not only an upstream component of the neurovascular response.

### 4.3. The baseline condition of the vasculature following BBB opening

Results from the ASL data used to measure baseline CBF indicate that there is no group average difference in resting blood flow between the left and right S1 regions for either the BBB Closed or the BBB Open condition. (Fig. 2). These measurements were performed between one and 2 h after the FUS plus microbubbles were used for BBB opening. This indicates that BBB opening does not put the vessels in the targeted region into a state of long-lasting dilation or constriction compared to non-targeted regions. Vessel constriction has been observed following FUS-BBB opening in both rats and mice, but it was shown to last only several minutes after which vessel diameter returned to the pre-FUS value (Cho et al., 2011; Raymond et al., 2007).

However, there is moderate evidence that baseline CBF is globally lower for the condition of BBB Open compared to BBB Closed. Baseline CBF values were higher by an average of 10% throughout the entire slice for the BBB Closed condition. Significant differences were only found when comparing the left and right S1 ROIs, which were averaged over nine voxels. If this is a real effect, it suggests a generalized effect on blood flow by the locally targeted FUS-BBB opening. It is known that diminished activity of the sympathetic nerves leads to decreases in blood flow (Sheng and Zhu, 2018). A number of processes may be considered to be involved in FUS induced changes in sympathetic tone: (1) Direct effects of BBB disruption: BBB dysfunction may decrease sympathetic excitatory function (Biancardi and Stern, 2016); (2) Cytokine release from BBB disruption, which may affect responsivity of sympathetic nerves (Elenkov et al., 2000; Kenney and Ganta, 2014); and (3) it is possible that the effects of FUS-BBB opening extended below the cortex and into subcortical autonomic centers that control blood flow.

It is also possible that the observed differences due were to uncontrolled changes in the experimental conditions between the two days that the BBB Closed and BBB Open imaging runs were performed on. For example, it is possible that the rats were under anesthesia for different time durations before the functional imaging runs, which could lead to them having been in different anesthetic states on average.

Here "resting blood flow" refers to times when there is no expected increase in flow due to stimulus-evoked activity. The baseline CBF maps were calculated by averaging together many time points over several minutes to give a single CBF value. They are not a dynamic series of CBF values over time, as are acquired in typical resting state fMRI studies. This is important as previous work from our group has shown that FUS BBB opening does alter inter-hemispheric resting state functional connectivity metrics as measured by BOLD fMRI (Todd et al., 2018). BBB opening must cause some alteration to the slow hemodynamic fluctuations that make up the resting state fMRI signal or effect the mechanisms that coordinate this signal between two physically separate brain regions. It is not clear what that alteration or effect would be.

### 4.4. Differences in non-targeted regions during BBB closed versus BBB open conditions

There is some ambiguous evidence that FUS-BBB opening might have non-local effects on the stimulus-evoked BOLD signal changes. The BOLD data for the non-targeted left S1 region presented in Fig. 3 show larger average changes in the BBB Open condition compared to the BBB Closed condition. The statistical evidence for these differences reaching significance is borderline – several time points in the 18-s stimulus data have uncorrected p-values slightly less than 0.01, but none of the time points in either the 6-s or 18-s data meet the criteria of $p < 0.05$ after correcting for multiple comparisons. Additionally, the effect of elevated BOLD signal changes in the non-targeted hemisphere during BBB opening was not observed in a previous study of ours that used a similar stimulus and BBB Closed vs BBB Open experimental conditions (Todd et al., 2019).

It is possible that the FUS-BBB opening targeted to the right hemisphere is somehow having an effect on the left hemisphere responses to stimulation. While we are unaware of a particular mechanism for such an effect, interhemispheric connections or brain autonomic responses may play a role in these observations. As with the differences seen in baseline CBF, it is possible that these observed differences are due to uncontrolled differences in the BBB Closed vs BBB Open experimental conditions.

### 4.5. Cortical depth dependence

The results from the high-resolution BOLD data looking at cortical depth effects are equivocal. The hypothesis behind the experiments was it might reveal something about the role of vessel retrograde signaling. Part of the neurovascular response is thought be a retrograde signaling mechanism that originates in the capillary bed and travels upstream in the vasculature via endothelial cells in order to recruit dilation from larger arterioles. FUS-BBB opening is known to disrupt tight junctions between endothelial cells (Sheikov et al., 2008) and therefore may weaken this signaling and result in a reduced increase in flow from diving arterioles and pial surface arteries. There was some evidence that the BOLD signal near the pial surface was even more attenuated than in the middle of the cortex in regions of BBB opening. But this effect was not consistent over all rats (Fig. 8 and Supplementary Figure S2), and the interpretation is somewhat complicated by the fact that this signal is also due to blood from draining veins.

### 4.6. Implications for non-contrast methods of BBB disruption detection

Beyond the physiological implications, a better understanding of this phenomenon may also have clinical implications if it can be used as a way to map the region of BBB disruption without the use of an exogenous contrast agent. Currently, the only method for determining the location and extent of BBB opening *in vivo* is with contrast weighted MRI imaging. This is acceptable for animal studies, but it would be preferable to not have to administer contrast to patients if avoidable. It is not immediately clear how a whole brain mapping of the observed effects due to BBB opening could be done. The most clearly observable effects where in the dynamic response to stimulus evoked neuronal activity. Such activation is localized and not possible to achieve in all brain regions. The use of a gas challenge will modulate flow in most of the brain. But it may not be feasible to ask sick patients to undergo such a process that puts a heavy burden on their breathing. Perhaps an imaging approach exists that was not considered in this study, e.g., (Gregori et al., 2013).

### 4.7. Conclusions and future directions

The present work reports that FUS-BBB opening diminishes the ability of cortical blood vessels to respond to demands for increased blood flow. This is not due to the vessels being in a state of continuous dilation or constriction, but rather some breakdown of the mechanisms that initiate and accomplish temporary vessel dilation. A specific mechanism still remains to be elucidated. At a gross level, no signs of histological damage were observed and the effect is transient and reversible. This study did not directly probe changes that may be occurring at the cellular or molecular levels. Information from further fMRI studies (e.g., cerebral blood volume measurements), additional types of experiments (e.g., immune responses, drug or receptor delivery) and imaging modalities (e.g. optical

imaging of blood vessels) will be needed to fully understand how FUS-BBB opening alters the neurovascular response. In addition to drug delivery studies, this work can also form a basis for evaluating neurological diseases that have as a basis opening or disruption of the BBB at more subtle levels.

## Conflicts of interest

The authors declare that they have no financial or non-financial competing interests related to this work.

## Acknowledgements

The research was supported by NIH grants K01EB023983, R01MG116858, and P01CA17464501. The authors would like to thank Natalia Vykhodtseva for her help in performing the histological analysis.

## Appendix A. Supplementary data

Supplementary data to this article can be found online at https://doi.org/10.1016/j.neuroimage.2019.116010.

## References

Adamczak, J.M., Farr, T.D., Seehafer, J.U., Kalthoff, D., Hoehn, M., 2010. High field BOLD response to forepaw stimulation in the mouse. Neuroimage 51, 704–712. https://doi.org/10.1016/j.neuroimage.2010.02.083.

Alsop, D.C., Detre, J.A., Golay, X., Günther, M., Hendrikse, J., Hernandez-Garcia, L., Lu, H., Macintosh, B.J., Parkes, L.M., Smits, M., Van Osch, M.J.P., Wang, D.J.J., Wong, E.C., Zaharchuk, G., 2015. Recommended implementation of arterial spin-labeled Perfusion mri for clinical applications: a consensus of the ISMRM Perfusion Study group and the European consortium for ASL in dementia. Magn. Reson. Med. 73, 102–116. https://doi.org/10.1002/mrm.25197.

Aryal, M., Arvanitis, C.D., Alexander, P.M., McDannold, N., 2014. Ultrasound-mediated blood-brain barrier disruption for targeted drug delivery in the central nervous system. Adv. Drug Deliv. Rev. 72, 94–109. https://doi.org/10.1016/j.addr.2014.01.008.

Aryal, M., Fischer, K., Gentile, C., Gitto, S., Zhang, Y.Z., McDannold, N., 2017. Effects on P-glycoprotein expression after blood-brain barrier disruption using focused ultrasound and microbubbles. PLoS One 12. https://doi.org/10.1371/journal.pone.0166061.

Biancardi, V.C., Stern, J.E., 2016. Compromised blood-brain barrier permeability: novel mechanism by which circulating angiotensin II signals to sympathoexcitatory centres during hypertension. J. Physiol. https://doi.org/10.1113/JP271584.

Brynildsen, J.K., Hsu, L.M., Ross, T.J., Stein, E.A., Yang, Y., Lu, H., 2017. Physiological characterization of a robust survival rodent fMRI method. Magn. Reson. Imaging 35, 54–60. https://doi.org/10.1016/j.mri.2016.08.010.

Burgess, A., Shah, K., Hough, O., Hynynen, K., 2015. Focused ultrasound-mediated drug delivery through the blood-brain barrier. Expert Rev. Neurother. https://doi.org/10.1586/14737175.2015.1028369.

Buxton, R.B., Wong, E.C., Frank, L.R., 1998. Dynamics of blood flow and oxygenation changes during brain activation: the balloon model. Magn. Reson. Med. 39, 855–864. https://doi.org/10.1002/mrm.1910390602.

Cho, E.E., Drazic, J., Ganguly, M., Stefanovic, B., Hynynen, K., 2011. Two-photon fluorescence microscopy study of cerebrovascular dynamics in ultrasound-induced blood-brain barrier opening. J. Cereb. Blood Flow Metab. 31, 1852–1862. https://doi.org/10.1038/jcbfm.2011.59.

Chu, P.-C., Liu, H.-L., Lai, H.-Y., Lin, C.-Y., Tsai, H.-C., Pei, Y.-C., 2015. Neuromodulation accompanying focused ultrasound-induced blood-brain barrier opening. Sci. Rep. 5, 15477. https://doi.org/10.1038/srep15477.

Chuang, K.H., van Gelderen, P., Merkle, H., Bodurka, J., Ikonomidou, V.N., Koretsky, A.P., Duyn, J.H., Talagala, S.L., 2008. Mapping resting-state functional connectivity using perfusion MRI. Neuroimage 40, 1595–1605. https://doi.org/10.1016/j.neuroimage.2008.01.006.

Elenkov, I.J., Wilder, R.L., Chrousos, G.P., Vizi, E.S., 2000. The sympathetic nerve–an integrative interface between two supersystems: the brain and the immune system. Pharmacol. Rev.

Gregori, J., Schuff, N., Kern, R., Günther, M., 2013. T2-based arterial spin labeling measurements of blood to tissue water transfer in human brain. J. Magn. Reson. Imaging 37, 332–342. https://doi.org/10.1002/jmri.23822.

Hynynen, K., McDannold, N., Sheikov, N.A., Jolesz, F.A., Vykhodtseva, N., 2005. Local and reversible blood-brain barrier disruption by noninvasive focused ultrasound at frequencies suitable for trans-skull sonications. Neuroimage 24, 12–20. https://doi.org/10.1016/j.neuroimage.2004.06.046.

Hynynen, K., McDannold, N., Vykhodtseva, N., Jolesz, F.A., 2001. Noninvasive MR imaging-guided focal opening of the blood-brain barrier in rabbits. Radiology 220, 640–646. https://doi.org/10.1148/radiol.2202001804.

Iadecola, C., 2017. The neurovascular unit coming of age: a journey through neurovascular coupling in health and disease. Neuron. https://doi.org/10.1016/j.neuron.2017.07.030.

Kenney, M.J., Ganta, C.K., 2014. Autonomic nervous system and immune system interactions. Comp. Physiol. https://doi.org/10.1002/cphy.c130051.

Kovacs, Z.I., Kim, S., Jikaria, N., Qureshi, F., Milo, B., Lewis, B.K., Bresler, M., Burks, S.R., Frank, J.A., 2017. Disrupting the blood–brain barrier by focused ultrasound induces sterile inflammation. Proc. Natl. Acad. Sci. 114, E75–E84. https://doi.org/10.1073/pnas.1614777114.

Lipsman, N., Meng, Y., Bethune, A.J., Huang, Y., Lam, B., Masellis, M., Herrmann, N., Heyn, C., Aubert, I., Boutet, A., Smith, G.S., Hynynen, K., Black, S.E., 2018. Blood–brain barrier opening in Alzheimer's disease using MR-guided focused ultrasound. Nat. Commun. 9. https://doi.org/10.1038/s41467-018-04529-6.

Mainprize, T., Lipsman, N., Huang, Y., Meng, Y., Bethune, A., 2019. Blood-brain barrier opening in primary brain tumors with non- invasive MR-guided focused Ultrasound : a clinical safety and feasibility study. Sci. Rep. 1–7. https://doi.org/10.1038/s41598-018-36340-0.

Marty, B., Larrat, B., Van Landeghem, M., Robic, C., Robert, P., Port, M., Le Bihan, D., Pernot, M., Tanter, M., Lethimonnier, F., Mériaux, S., 2012. Dynamic study of blood-brain barrier closure after its disruption using ultrasound: a quantitative analysis. J. Cereb. Blood Flow Metab. 32, 1948–1958. https://doi.org/10.1038/jcbfm.2012.100.

McDannold, N., Vykhodtseva, N., Hynynen, K., 2006. Targeted disruption of the blood-brain barrier with focused ultrasound: Association with cavitation activity. Phys. Med. Biol. https://doi.org/10.1088/0031-9155/51/4/003.

Meairs, S., 2015. Facilitation of drug transport across the blood-brain barrier with ultrasound and microbubbles. Pharmaceutics 7, 275–293. https://doi.org/10.3390/pharmaceutics7030275.

Muoio, V., Persson, P.B., Sendeski, M.M., 2014. The neurovascular unit - concept review. Acta Physiol. https://doi.org/10.1111/apha.12250.

O'Reilly, M.A., Muller, A., Hynynen, K., 2011. Ultrasound insertion loss of rat parietal bone appears to Be proportional to animal mass at submegahertz frequencies. Ultrasound Med. Biol. https://doi.org/10.1016/j.ultrasmedbio.2011.08.001.

Park, J., Zhang, Y., Vykhodtseva, N., Jolesz, F.A., McDannold, N.J., 2012. The kinetics of blood brain barrier permeability and targeted doxorubicin delivery into brain induced by focused ultrasound. J. Control. Release 162, 134–142. https://doi.org/10.1016/j.jconrel.2012.06.012.

Paxinos, G., Watson, C., 2013. Rat Atlas sixth ed. J. Chem. Inf. Model. https://doi.org/10.1017/CBO9781107415324.004.

Raymond, S.B., Skoch, J., Hynynen, K., Bacskai, B.J., 2007. Multiphoton imaging of ultrasound/Optison mediated cerebrovascular effects in vivo. J. Cereb. Blood Flow Metab. 27, 393–403. https://doi.org/10.1038/sj.jcbfm.9600336.

Sheikov, N., McDannold, N., Sharma, S., Hynynen, K., 2008. Effect of focused ultrasound applied with an ultrasound contrast agent on the tight junctional integrity of the brain microvascular endothelium. Ultrasound Med. Biol. 34, 1093–1104. https://doi.org/10.1016/j.ultrasmedbio.2007.12.015.

Sheikov, N., McDannold, N., Vykhodtseva, N., Jolesz, F., Hynynen, K., 2004. Cellular mechanisms of the blood-brain barrier opening induced by ultrasound in presence of microbubbles. Ultrasound Med. Biol. 30, 979–989. https://doi.org/10.1016/j.ultrasmedbio.2004.04.010.

Sheng, Y., Zhu, L., 2018. The crosstalk between autonomic nervous system and blood vessels. Int. J. Physiol. Pathophysiol. Pharmacol.

SPM12, 2014. SPM12 Framework ([WWW Document]).

Tian, P., Teng, I.C., May, L.D., Kurz, R., Lu, K., Scadeng, M., Hillman, E.M.C., De Crespigny, A.J., D'Arceuil, H.E., Mandeville, J.B., Marota, J.J.A., Rosen, B.R., Liu, T.T., Boas, D.A., Buxton, R.B., Dale, A.M., Devor, A., 2010. Cortical depth-specific microvascular dilation underlies laminar differences in blood oxygenation level-dependent functional MRI signal. Proc. Natl. Acad. Sci. 107, 15246–15251. https://doi.org/10.1073/pnas.1006735107.

Timbie, K.F., Mead, B.P., Price, R.J., 2015. Drug and gene delivery across the blood-brain barrier with focused ultrasound. J. Control. Release 219, 61–75. https://doi.org/10.1016/j.jconrel.2015.08.059.

Todd, N., Zhang, Y., Arcaro, M., Becerra, L., Borsook, D., Livingstone, M., McDannold, N., 2018. Focused ultrasound induced opening of the blood-brain barrier disrupts inter-hemispheric resting state functional connectivity in the rat brain. Neuroimage 178, 414–422. https://doi.org/10.1016/j.neuroimage.2018.05.063.

Todd, N., Zhang, Y., Power, C., Becerra, L., Borsook, D., Livingstone, M., McDannold, N., 2019. Modulation of brain function by targeted delivery of GABA through the disrupted blood-brain barrier. Neuroimage 189, 267–275. https://doi.org/10.1016/j.neuroimage.2019.01.037.

Valdés-Hernández, P.A., Sumiyoshi, A., Nonaka, H., Haga, R., Aubert-Vásquez, E., Ogawa, T., Iturria-Medina, Y., Riera, J.J., Kawashima, R., 2011. An in vivo MRI template set for morphometry, tissue segmentation, and fMRI localization in rats. Front. Neuroinf. 5, 26. https://doi.org/10.3389/fninf.2011.00026.